Protic NHC Iridium Complexes with beta-H Reactivity-Synthesis, Acetonitrile Insertion, and Oxidative Self-Activation

Rong, Mark K.

2019-12-09

Rong , M K , Chirila , A , Franciolus , D , Lutz , M , Nieger , M , Ehlers , A W , Slootweg , J C & Lammertsma , K 2019 , ' Protic NHC Iridium Complexes with beta-H Reactivity-Synthesis, Acetonitrile Insertion, and Oxidative Self-Activation ' , Organometallics , vol. 38 , no. 23 , pp. 4543-4553 . https://doi.org/10.1021/acs.organomet.9b00584

http://hdl.handle.net/10138/309063
https://doi.org/10.1021/acs.organomet.9b00584

ORGANOMETALLICS

Article

Cite This: Organometallics 2019, 38, 4543−4553

pubs.acs.org/Organometallics

Protic NHC Iridium Complexes with β-H Reactivity−Synthesis, Acetonitrile Insertion, and Oxidative Self-Activation

Mark K. Rong,[†] Andrei Chirila,[†] David Franciolus,[†] Martin Lutz,[‡] Martin Nieger,[§] Andreas W. Ehlers,[†,∥,⊥] J. Chris Slootweg,*[,†,⊥] and Koop Lammertsma*[,†,∥]

[†]Department of Chemistry and Pharmaceutical Sciences, Vrije Universiteit Amsterdam, De Boelelaan 1083, 1081 HV Amsterdam, The Netherlands

[‡]Crystal and Structural Chemistry, Bijvoet Center for Biomolecular Research, Utrecht University, Padualaan 8, 3584 CH Utrecht, The Netherlands

[§]Department of Chemistry, University of Helsinki, A. I. Virtasen aukio 1, P.O. Box 55, Helsinki, Finland

[∥]Department of Chemistry, Oakland Park 2006University of Johannesburg, Johannesburg 2006, South Africa

Supporting Information

ABSTRACT: Protic NHC iridium complexes, obtained from the corresponding azido-phenylene-isocyanide precursor complexes, were investigated for ligand-based reactivity. Under redox-neutral conditions, acetonitrile inserts into the N−H bonds to provide κ^2-NHC-imidoyl ligand-based complexes, while under reductive conditions the complex also expels one N−H proton to provide the corresponding deprotonated analogues. Using zinc as a reductor activates the NHC-iridium complex to form an asymmetric bimetallic iridium hydrido complex, in which two anionic N-deprotonated NHCs bridge the bimetallic core. X-ray crystal structures are reported for the azido-phenylene-isocyanide precursor complex, the protic NHC complex, and the asymmetric bimetallic iridium hydride complex. Density functional computations and a QTAIM analysis of the bimetallic iridium hydrido complex are provided.

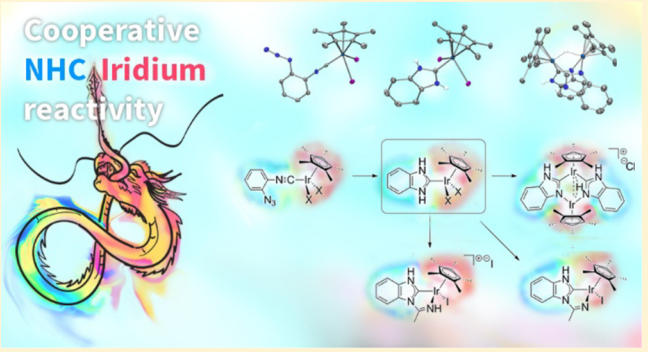

INTRODUCTION

Since 1968,[1,2] N-heterocyclic carbenes (NHCs) have been prominent ligands of high stability with robust coordination chemistry. Protic NHCs (hereafter NHC^{H}s) were first introduced in the 1980s,[3] but only recently has their chemistry become widely accessible through the syntheses of Hahn et al.[4] These synthetic routes conveniently mitigate the inherent acidic reactivity of the NHC^H-NH sites, which contrast with the classical nonreactive N-substituted NHCs.[5] This protic character enables hydrogen-bonding interactions, deprotonations, and nucleophilic additions and highlights the ability of NHC^{H}s to act as "cooperative" or "non-innocent" ligands.[6,7] For instance, H-bonding increases substrate recognition in the competitive Rh(I)-catalyzed hydrogenation of esters[8] and assists in the Ru(II)-catalyzed condensation of allyl alcohols with 2-pyridylbenzimidazole.[9] Deprotonation of the NHC^H provides an N-anionic ligand which can be used to access nonsymmetrical NHCs (Scheme 1) and macromolecular structures[4,10,11] or to bind a second metal center (Figure 1).[12−16] These multimetallic structures generally bear their bridging NHCs in a head-to-tail fashion and are of interest for multinuclear catalysis.[17] Deprotonated NHC N sites have been used in ruthenium(II) complexes for bifunctional activation of amines, dihydrogen, and alcohols, as demonstrated in the catalytic transfer hydrogenation of acetophenone using *i*-PrOH.[18] Iridium(III) NHC^H complexes have shown bifunctional activation of dihydrogen and acetylene.[19] NHC^H deprotonation has been suggested to be facilitated by intramolecular ligand−metal interactions,[9,20] indicating the importance of the nature of the transition metal. For instance, NHC^{H}s can be transformed to the imidazole form by an external base,[13] but in the 2-functionalization of imidazoles by Ru(II)[9] and Rh(I) catalysts[20] the tautomerization results from ligand-β-H activation by the metal, presumably via metal-hydride intermediates (Scheme 2).[20,21] Metal-mediated NHC^H reactivity can also be induced by free coordination sites. Illustrative is the chloride displacement on iridium(III) that

Scheme 1. Ligand-Based NHC Reactivity

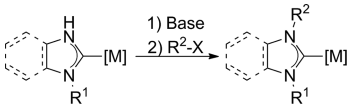

Received: August 27, 2019
Published: November 19, 2019

DOI: 10.1021/acs.organomet.9b00584
Organometallics 2019, 38, 4543−4553

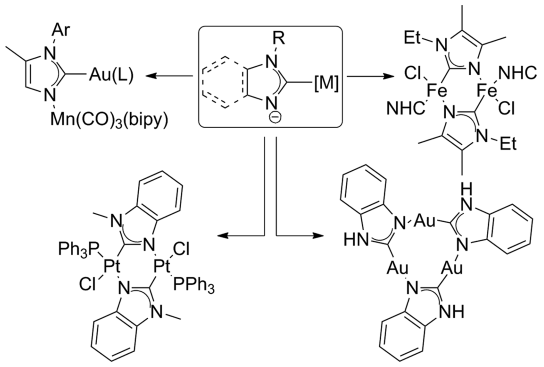

Figure 1. N-anionic protic NHC coordination chemistry.

Scheme 2. NHC^H Tautomerization Step by Intramolecular Interaction with Catalyst

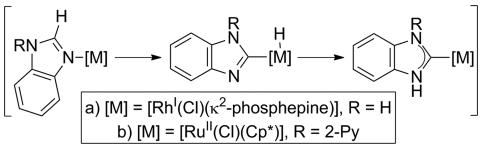

facilitates a nucleophilic attack of the NHC^H on a coordinated MeCN molecule to stoichiometrically provide a formal hydroamination product, which rearranges to a bis(imidazole) complex (Scheme 3).[22−24] Collectively, these examples demonstrate the versatile chemistry of NHC^H complexes.

Scheme 3. Capture of MeCN by Protic NHC Followed by Tautomerization

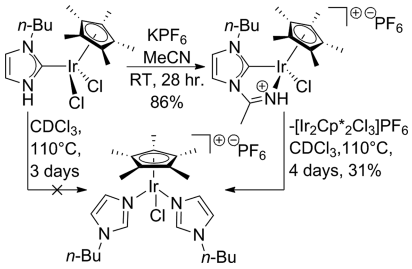

NHC^{H}s can also differ electronically from their N-substituted analogues. The prominence of NHCs in organometallic catalysis is generally attributed to their strong σ donation, but NHCs can also be tunable π acceptors.[25,26] In a computational study on NHC-phosphinidene complexes,[27,28] we found the conformation of the NHC to be crucial for its electronic behavior in the complex. For example, the N-methylated NHC in Ru complex **A** favors the σ-donating orthogonal ⊥ arrangement over the coplanar ∥ arrangement by 12.5 kcal mol^{-1}, but the sterically less encumbered protic NHC in **B** favors instead a coplanar ∥ conformation by 2.5 kcal mol^{-1} (Figure 2),[29] thereby allowing for significant π-acceptor capacity due to increased phosphinidene-NHC orbital overlap. This unique effect of the NHC^H ligand is even more pronounced in benzimidazolidin-2-ylidene iridium complexes as NHC^{Me} complex **C**⊥ is favored by 22.0 kcal mol^{-1}, while NHC^H complex **D**∥ is favored by 3.4 kcal mol^{-1} (Figure 2).[30−33] These results prompted us to study NHC^H iridium complexes and assess the effect of the ligand on the complex's overall reactivity. We address the distinct coordination

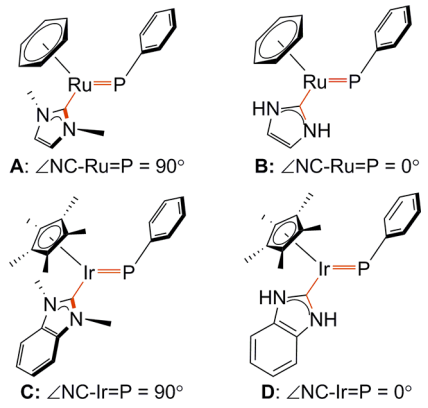

Figure 2. NHC conformations with different electronic effects.

parameters of NHC^H iridium(III) complexes and then explore the reactivity of their β-NH groups in stoichiometric hydroamination-type activations, as well as in self-activation under reductive conditions toward a unique bimetallic structure.

RESULTS AND DISCUSSION

The syntheses and properties of the NHC^H iridium complexes are discussed first. Next, their reactivity toward MeCN is explored under both redox-neutral and reductive conditions. Finally, the NHC^H reactivity will be addressed in an oxidative reaction to examine the influence of an N-anionic NHC^H on the formation of a dinuclear complex. Computational methodologies are used to provide background for the observed reactivity.

Synthesis of NHC^H Ir(III) Complexes. The synthesis of the NHC^H iridium(III) complexes was pursued in analogy to that reported for the related ruthenium(II) complexes, in which 2-azido-isonitrile precursors are reduced to amino-isonitrile intermediates that then cyclize.[34] Reacting 2-azidophenylisonitrile (**1**)[35] with 0.5 equiv of [IrCp*Cl$_2$]$_2$ in DCM at room temperature provided [(2-azidophenylisonitrile)IrCp*Cl$_2$] precursor complex **2** in 98% isolated yield as a light-sensitive yellow powder (Scheme 4).

Scheme 4. Synthesis of Protic NHC-Iridium Complex 4

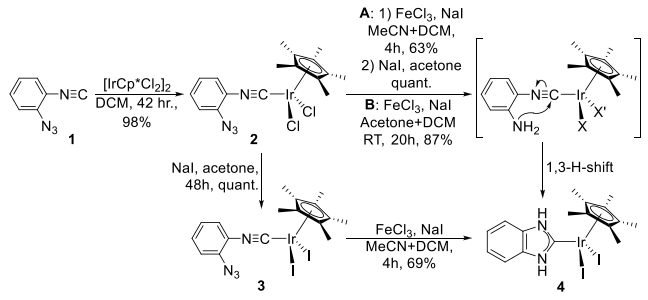

Whereas **2** was stable as a solid in darkness for months, it slowly decomposed in solution, even at −80 °C. To allow for full analysis, **2** was treated with NaI in acetone to quantitatively provide the thermally stable diiodo complex **3**. Suitable crystals for an X-ray crystal structure determination were obtained by slow diffusion of pentane into a DCM solution. The molecular structure of **3** shows a linear isocyanide with a C1−N1 triple-bond length of 1.159(3) Å (Figure 3). The Ir−C1 bond length

DOI: 10.1021/acs.organomet.9b00584
Organometallics 2019, 38, 4543−4553

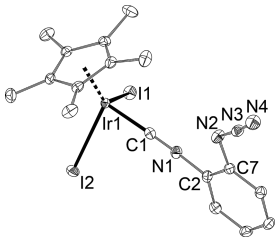

Figure 3. Displacement ellipsoid plot of iridium complex **3** at the 50% probability level. Hydrogen atoms and DCM solvent molecules are omitted for clarity. Selected bond lengths (Å) and angles (deg): Ir1−C1 = 1.922(2), Ir1−I1 = 2.6965(3), Ir1−I2 = 2.6965(3), C1−N1 = 1.159(3), N1−C2 = 1.390(3), C2−C7 = 1.401(3), C7−N2 = 1.416(3), N2−N3 = 1.254(3), N3−N4 = 1.125(3), C1—N2 = 3.445(3), N1−C1−Ir1 = 177.6(2), C1−N1−C2 = 177.2(2), C2−C7−N2 = 115.9(2), N4−N3−N2 = 172.8(3), I1−Ir1−I2 = 90.709(7), C2−C7−N2−N3 = 178.0(2).

of 1.922(2) Å compares well to those of other (aryl)-isocyanide-iridium(III) complexes,[36] as do the iridium−iodide bond lengths (Ir1−I1 = 2.6965(3); Ir1−I2 = 2.6965(3) Å).[36a] The distance of 3.445(3) Å between the C1 and N2 atoms together with the C2−C7−N2−N3 torsion angle of 178.0(2)° illustrate the prearrangement of N2 for nucleophilic attack on C1 in the subsequent reduction step (vide infra). The structural parameters of the isocyanide ligand compare also well with those reported for [**1**-W(CO)$_5$].[35]

Reduction of the azide group of **2** to the corresponding amine induces cyclization to the desired NHC^H complex (Scheme 4).[34,37] This was accomplished by reaction with NaI and $FeCl_3$ in DCM and MeCN for 4 h,[38] after which quenching and purification of the black reaction mixture provided the desired diiodo complex **4** as a yellow solid in 63% yield (δ(^{1}H) 9.88 (N*H*); δ(^{13}C) 161.0 (N*C*N) ppm) (**A** in Scheme 4). The chloride to iodide exchange that occurs on iridium results from the excess of NaI that is required for the azide reduction.[39] This exchange can also be performed prior to the reduction step: i.e., **2** → **3** → **4**. The best results were obtained by performing the azide reduction in a mixture of acetone/DCM over 20 h at room temperature (**B** in Scheme 4) to provide **4** in higher purity and yield (87%).

For completeness, we note that the chloride to iodide exchange on iridium can easily be reversed (Scheme 5); to the

Scheme 5. Iodide to Chloride Ion Exchange

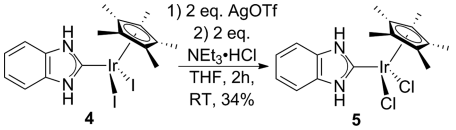

best of our knowledge, such a protocol is still undocumented. Thus, reacting **4** with 2 equiv of AgOTf in THF provides a bright yellow bis(triflate) complex, which on treatment with NEt_3·HCl as chloride donor turned orange, which indicates the formation of the dichloro complex. Purification and crystallization provided **5** as orange needles (34%; δ(^{1}H) 10.52 (N*H*); δ(^{13}C) 165.7 (N*C*N) ppm).

Next, we compared the properties of NHC^H complex **4** with those of NHC^{Me} analogue **6**, which was obtained by coordinating bis(1,3-dimethylbenzimidazolidin-2-ylidene)[40] to [IrCp*Cl$_2$]$_2$ (88%) and subsequent Cl → I ion exchange using NaI (quantitative, Scheme 6). The ^{13}C NMR spectra showed

Scheme 6. Synthesis of Me-Substituted NHC-Ir Complex 6

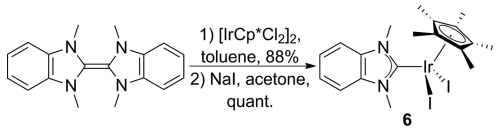

an upfield shift for the NCN carbene carbon of the NHC^H complex (**4**, δ 161.0 ppm; **6**, δ 167.0 ppm), similar to the trend for comparable Pd[10a] complexes, and is suggestive of a stronger C−Ir interaction,[41] which could be confirmed by comparing the molecular structures obtained from X-ray structure determinations (Figure 4). Red crystalline needles of **4** were

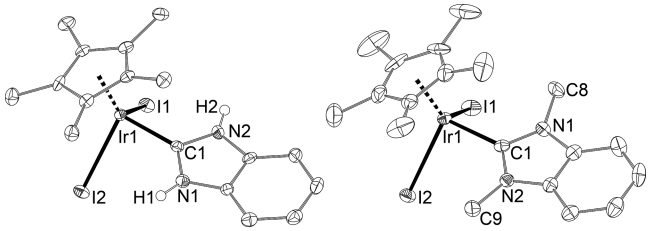

Figure 4. Displacement ellipsoid plots of iridium complexes **4** (left) and **6** (right) at the 50% probability level. C−H hydrogen atoms are omitted for clarity. Selected bond lengths (Å) and angles (deg) of **4**: Ir1−C1 = 2.008(4), Ir1−I1 = 2.6964(4), Ir1−I2 = 2.6982(4), C1−N1 = 1.338(6), C1−N2 = 1.355(6), N1−C1−N2 = 106.2(4), N1−C1−Ir1 = 127.0(3), N2−C1−Ir1 = 126.0(3), I1−Ir1−I2 = 90.381(11). Selected bond lengths (Å) and angles (deg) of **6**: Ir1−C1 = 2.034(4), Ir1−I2 = 2.7254(3), Ir1−I1 = 2.7284(3), C1−N1 = 1.361(5), C1−N2 = 1.370(5), N1−C8 = 1.453(5), N2−C9 = 1.457(5), N1−C1−N2 = 105.0(3), N1−C1−Ir1 = 126.9(3), N2−C1−Ir1 = 127.1(3), I2−Ir1−I1 = 86.008(10).

obtained by slow diffusion of pentane into a DCM solution and those of **6** from DCM/pentane at 5 °C. The molecular structures show a near-C_s symmetry, an identical NHC conformation and parameters comparable to those of related Ir-NHC complexes,[42] with indeed a shorter iridium−carbene bond length for the protic complex (**4**, Ir1−C1 = 2.008(4) Å; **6**, Ir1−C1 = 2.034(4) Å) and a larger I1−Ir1−I2 bond angle (**4**, 90.381(11)°; **6**, 86.008(10)°). These differences may be the result of the sterically smaller N substituents of **4** (see Figure S35 in the Supporting Information) or the observed intermolecular NH−I hydrogen bonds (H1—I2' 2.86(3); H2—I2" 2.85(2) Å).[43] ETS-NOCV[44] fragment analysis on BP86-D3(ZORA)/TZ2P[32,33] optimized structures of **4** and **6** revealed tighter orbital interactions for the NHC^H ligand (E_{Ir-C}^4 = −114.1 kcal mol^{-1}; E_{Ir-C}^6 = −106.2 kcal mol^{-1}), due to significant donation from the carbene to the metal (E_σ^4 = −90.6 kcal mol^{-1}, E_σ^6 = −82.6 kcal mol^{-1}), as well as back-donation to the carbene p orbital ($E_{\pi 1}^4$ = −16.6 kcal mol^{-1}, $E_{\pi 1}^6$ = −15.4 kcal mol^{-1}) and the C═N antibonding orbitals ($E_{\pi 2}^4$ = −6.9 kcal mol^{-1}, $E_{\pi 2}^6$ = −8.2 kcal mol^{-1}). The possibility of a 90° rotation in the NHC conformation and the effect thereof on the electronic parameters was examined as well and appeared to be more accessible for the protic complex **4** (maxima: $\Delta E_{\perp\rightarrow\parallel}^4$ = +3.7 kcal mol^{-1}; $\Delta E_{\perp\rightarrow\parallel}^6$ = +13.4 kcal mol^{-1}), which weakens the Ir−C bond (E_{Ir-C} = −110.4 kcal mol^{-1}; E_σ = −86.5 kcal mol^{-1}, $E_{\pi 1}$ = −17.2 kcal mol^{-1}, $E_{\pi 2}$ = −6.7 kcal mol^{-1}). Thus, the accessible coplanar conformation and observed hydrogen bonding sets the protic NHC apart

DOI: 10.1021/acs.organomet.9b00584
Organometallics 2019, 38, 4543−4553

from its N-methylated analogue. The stronger Ir−C bond is favorable for anchoring the ligand firmly for followup reactions.

NHC^H MeCN Activation. Next, stoichiometric hydroamination-type activation by the protic NHC^H-Ir complex was assessed.[22] Refluxing **4** for 24 h in MeCN resulted in the nitrile's insertion into one of the ligand's N−H bonds to quantitatively afford **7** as an unstable yellow solid (Scheme 7).

Scheme 7. Protic NHC-NH Addition over the MeCN Triple Bond and DFT Analysis of [7*]$^+$ and [7]$^+$

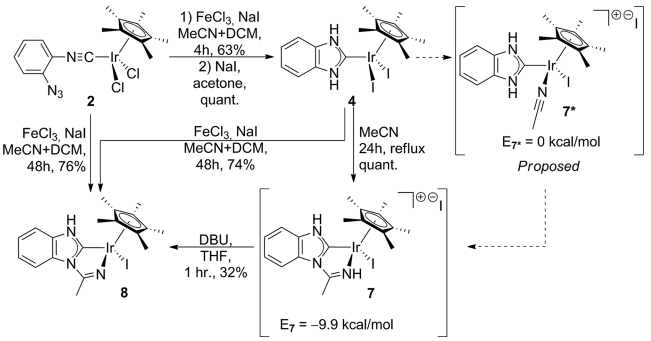

The product's asymmetrically substituted benzimidazolin-2-ylidene ligand is evident from the two different NH groups in the ^{1}H NMR spectrum (δ 13.08, 10.88 ppm). BP86-D3(ZORA)/TZ2P calculations[32,33] indicate that, upon MeCN coordination (**7***), the addition of the NHC^H−NH bond to the CN triple bond to give **7** is exothermic by 9.9 kcal mol^{-1} (Scheme 7). No full characterization by ^{13}C NMR or an X-ray structure determination could be performed, as isolated **7** quickly converted into an intractable solid, which we presume to be the (benzimidazolyl)IrCp*I$_2$ tautomer.[45]

We wondered whether **7** also forms directly from precursor **2** in a one-pot reaction. However, increasing the reaction time for the $FeCl_3$/NaI-facilitated reduction to 48 h provided instead exclusively the deprotonated bidentate [(imidoyl-NHC^H)IrI] complex **8** (76%, Scheme 7). Its ^{1}H NMR spectrum showed one N−H resonance (δ 7.94 ppm) and an asymmetrically substituted benzimidazolin-2-ylidene with chemical shifts that differ from those of **7** (see Figure S30 in the Supporting Information) and distinctive carbene and imidoyl ^{13}C NMR resonances (δ 171.6 (NCN), 164.6 (*C*NH) ppm). The same product was obtained by deprotonating **7** with DBU in THF (1 h, room temperature, 32%). In contrast to **7**, **8** is stable in air and water. Exposure of intermediate **4** to $FeCl_3$/NaI for 48 h in MeCN yielded the same complex **8** (74%; Scheme 7). This suggests that the reductive reaction medium causes the loss of 1 equiv of HI from **4**, since no deprotonating base is present. The activator could be Fe(II), which is generated in situ on mixing $FeCl_3$ and NaI in solution.[38,46]

The observed insertion reactivity in complexes **7** and **8** may have potential in catalysis. Since the products are reminiscent of iminium ions (i.e., nitrogen-stabilized N-protic nitrilium ions), which readily undergo nucleophilic attack,[47] this might be exploited in the (catalytic) functionalization of nitriles or terminal triple bonds.[23,48] Alternatively, **7** and **8** could serve as, for instance, [(κ^2-imidoyl-aryl)Ir^{III}] transfer hydrogenation catalysts.[49] Overall, it is especially interesting that the reactivity of the NHC^H complex changes upon reduction. To better understand the role of the metal center in this, we continued using a well-defined iridium reductor.

NHC^H β-Deprotonation to Dinuclear Complex. The conversion of **4** to **8** occurred under reductive conditions. Since zinc is a well-known reductor for iridium(III) chlorides[50] and compatible with NHC^{H}s,[51] we decided to explore it for enhanced NH−metal interactions with surprising results. When dichloro complex **5** was refluxed in MeOH for 7 days in the presence of Zn, the μ-hydrido dinuclear complex **9** was obtained as an unexpected product (Scheme 8); no reaction

Scheme 8. Formation of Dinuclear Complex 9

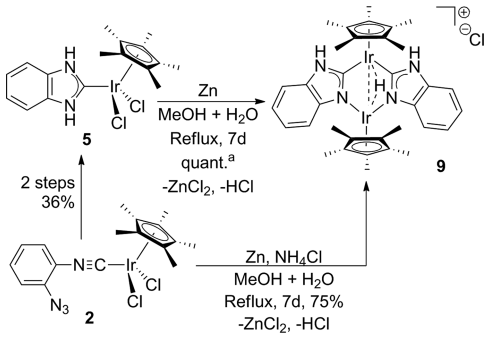

[a]NMR yield.

took place in the absence of Zn. Complex **9** also resulted directly from **2** in 75% yield by refluxing in MeOH/H_2O for 7 days in the presence of Zn and NH_4Cl. This method is more efficient than the three-step approach (36%).

Complex **9** has a unique C_s symmetry with two anionic NHC ligands and a hydride bridging its iridium atoms (δ(^{1}H) −20.01 ppm).[52] While bimetallic iridium species with bridging hydride ligands are well-known,[42,53−57] those with bridging NHC ligands are rare and tend to have them coordinated in a head-to-tail fashion between identical metal centers.[12−16] In contrast, **9** features a head-to-head arrangement with inequivalent Ir centers. This is supported by two distinct Cp*-CH_3 ^{1}H and ^{13}C NMR chemical shifts (δ(^{1}H) 2.23, 2.15; δ(^{13}C) 11.8, 10.9 ppm). NOESY measurements show coupling of one Cp* ligand with the two NHC N-hydrogens and coupling of the other Cp* ligand with the nearby aromatic N$^-$-CC*H* hydrogens (see the Supporting Information). The two carbene ^{13}C NMR resonances of **9** are considerably more upfield than that of **5** (**9**: δ 142.2 ppm; **5**, δ 165.7 ppm), which is attributed to the higher shielding in the anionic NHC.

An X-ray crystal structure determination established unequivocally the molecular structure of **9** (Figure 5). Single crystals were obtained by slow diffusion of diethyl ether into a DCM solution in the presence of TPPO.[58,59] The two independent molecules in the asymmetric unit of **9** are located on general positions without crystallographic symmetry. The iridium−carbene distances are similar to those in mononuclear **4** (**9**, Ir11−C11 = 2.016(7) Å, Ir11−C81 = 2.020(7) Å, Ir12−C12 = 2.038(7) Å, Ir12−C82 = 2.014(7) Å; **4**, Ir1−C1 = 2.008(4) Å), and the nitrogen−iridium bond lengths (Ir21−N11 = 2.083(6) Å, Ir21−N31 = 2.088(6) Å, Ir22−N12 2.072(6) Å, Ir22−N32 2.078(7)Å) are comparable to those found in structurally similar iridium imidazolate and pyrazolate complexes.[55,60] The location of the μ-hydride could not be determined from difference-Fourier maps, but its calculated position was evident from the geometry of the iridium centers.

The intriguing bonding in the metallic core of **9**, with its bridging hydride and delocalized anionicity of the NHC

DOI: 10.1021/acs.organomet.9b00584
Organometallics 2019, 38, 4543−4553

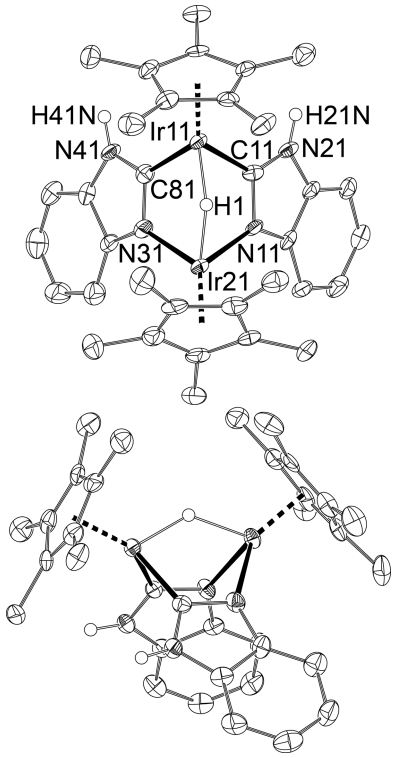

Figure 5. Displacement ellipsoid plots of dinuclear iridium complex **9** at the 50% probability level. Only one of the two independent molecules is shown. C−H hydrogen atoms, the chloride anion, and DCM solvent molecules are omitted for clarity. Selected bond lengths (Å) and angles (deg): Ir11−C11 = 2.016(7), Ir11−C81 = 2.020(7), Ir21−N11 = 2.083(6), Ir21−N31 = 2.088(6), N11−C11 = 1.344(9), N21−C11 = 1.351(9), N31−C81 = 1.341(9), N41−C81 = 1.349(9), Ir11—Ir21 = 3.0410(4), C11−Ir11−C81 = 81.0(3), N11−Ir21−N31 = 80.0(2). Atom H1 was introduced in a calculated position.

ligands, makes the oxidation states of the metal centers ambiguous[56] (i.e., Ir(III)—Ir(III), Ir(II)—Ir(IV), or Ir(II)→Ir(IV)). Intermetallic interaction between the two Ir centers seems arguable[54−57] because of the rather large separation (Ir11—Ir21 = 3.0410(4), Ir12—Ir22 = 3.0501(4) Å). Since the low solubility of **9** prevented CV measurements, we used a QTAIM analysis[61] on a BP86-D3(ZORA)/TZ2P[32,33] optimized geometry, which showed near-identical bond paths of the two iridium nuclei to the hydride (critical bond points Ir11−H1 ρ 0.12 au, ε 0.09, Ir21−H1 ρ 0.10 au, ε 0.08; ring critical points Ir11−H1−Ir21−N31−C81: ρ 0.03 au, Ir11−H1−Ir21−N11−C11: ρ 0.03 au) but no intermetallic interactions (Figure 6 and Figure S36 in the Supporting Information). This indicates true hydride bridging and minimal electronic differences between the Ir nuclei: i.e., a Ir(III)/Ir(III) complex.[62]

The unique NHC^H orientation in **9** was examined computationally, since it contrasts with that of known NHC-bridged complexes.[12−16] The head-to-head coordination of complex **9** is indeed energetically favored at the BP86-D3(ZORA)/TZ2P level[32,33] over head-to-tail complex **10**, but by only 1.9 kcal mol^{-1} (Figure 7). This small energy difference is somewhat surprising, since ^{1}H NMR spectra of the crude reaction mixtures show full selectivity of its formation. For the formation of **9** from the monometallic precursor, one NHC ligand has to undergo an in situ tautomerization, either prior to or after coordination to the second Ir center. Considering that

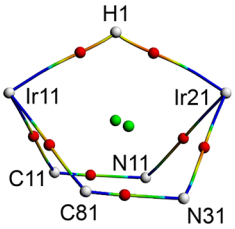

Figure 6. AIM analysis of bond paths in **9**. NHC and Cp* ligands are omitted for clarity. Bond critical points are shown in red and ring critical points in green.

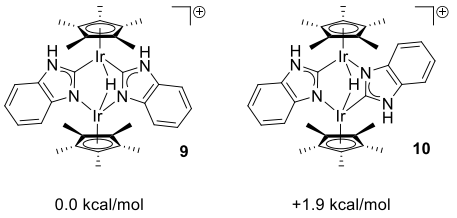

Figure 7. Relative BP86-D3(ZORA)/TZ2P energies of **9** and tautomer **10**.

zinc is essential for the conversion, we presume it oxidizes to $ZnCl_2$ to facilitate the Ir(III) → Ir(I) reduction of one monometallic complex, which then undergoes an auto-oxidative 1,3-H shift to the corresponding hydride complex, as has been reported for alkyl-iridium(III) hydrides.[63] NHC tautomerization is likely for Ir(I) complexes bearing ligands with a strong trans effect, such as hydrides.[21,64] Such an oxidative addition−tautomerization sequence has also been suggested for benzimidazole-Ru-hydrides (DFT).[21b] It should be noted that the tautomerization step may also be influenced by the second metal center, as was found for Au/Mn-NHC systems.[13]

The observed oxidative activity leading to **9** seems to be specific for iridium; using [Rh^{III}Cp*Cl$_2$] and [Ru^{II}(p-cym)-Cl$_2$][34] in the same one-pot procedure resulted in a mixture of Rh and Ru analogues of **5** with unidentified side products (see the Supporting Information). The Ir-chloride atoms are essential, as the diiodo complexes **3** and **4** gave no conversion. This halide-specific reactivity may be attributed to the difference in redox potentials or alternatively be related to a difference in H-bonding interactions that can assist 1,3-H shifts in iridium hydrides.[63]

CONCLUSION

Using a robust route from azido-phenylene-isocyanide precursor complexes, we obtained NHC^H Ir(III) complexes. The reactivity of the NHC N−H group in these complexes could be enhanced under reductive conditions, which is suggestive of a metallophilic interaction (β-H activation) that distinguishes it from reported base-induced reactions. The reactivity was used to access various unique complexes. The NHC^H could nucleophilically attack MeCN to provide neutral κ^2-NHC-imidoyl ligands and under reductive conditions their anionic analogues, which both are interesting ligands for catalysis. In the presence of zinc, the NHC^H iridium chloride complex underwent oxidative self-activation, which resulted in the formation of an unprecedented C_s-symmetric dinuclear iridium hydride complex, bearing two head-to-head coordinated bridging N-deprotonated NHCs. Overall, it is exciting to

DOI: 10.1021/acs.organomet.9b00584
Organometallics 2019, 38, 4543−4553

observe that the reactivity of the NHC^Hs changes upon reduction of the complex. It may lead to new applications for these ligands, prove helpful in understanding the mechanistic steps for NHC^H catalysts, and, as such, further the development of NHCs as cooperative ligands.

EXPERIMENTAL SECTION

Computational Procedures. Density functional calculations were performed at the BP86/ZORA/Grimme-D3/TZ2P level of theory[32] using the Amsterdam Density Functional (ADF)[33] 2013.01 (geometry optimizations, QTAIM[60]) and 2016.102 (ETS-NOCV[43]). The nature of each stationary point was confirmed by frequency calculations.

Preparation of Compounds. All experiments were performed under an atmosphere of dry nitrogen using standard Schlenk-line and glovebox techniques, unless stated otherwise. Solvents were distilled under nitrogen over the appropriate drying agent: $CaCl_2$ (DCM), benzophenone/NaK (Et_2O, THF), $LiAlH_4$ (pentane), K_2CO_3 (MeCN, acetone), P_2O_5 (CD_2Cl_2, $CDCl_3$). Anhydrous MeOH was obtained from Sigma-Aldrich. Water was degassed ultrasonically under reduced pressure. 2-Azidophenyl isonitrile (**1**)[35] was kindly provided by C. A. Dumke and F. E. Hahn.[65] (1,2,3,4,5-Pentamethylcyclopentadienyl)iridium(III) dichloride dimer,[66] 1,3-dimethylbenzimidazolium iodide,[67] bis(1,3-dimethylbenzimidazolidin-2-ylidene),[40] and (2-azidophenylisonitrile)(1-methyl-4-isopropylbenzene)ruthenium(II) dichloride[34] were prepared according to literature procedures. All other reagents were used as received. Solids were predried in vacuo for at least 15 min. NMR spectra were recorded on Bruker Avance 400 (^{1}H, 400.13 MHz; $^{13}C\{^1H\}$, 100.61 MHz, room temperature) or a Bruker Avance 500 (^{1}H, 500.23 MHz; $^{13}C\{^1H\}$, 125.78 MHz; room temperature). Chemical shifts are reported in ppm downfield from tetramethylsilane. ^{1}H spectra were internally referenced to residual solvent resonances: $CDCl_3$ (δ 7.26) and CD_2Cl_2 (δ 5.32). ^{13}C spectra were internally referenced to residual solvent resonances: $CDCl_3$ (δ 77.16) and CD_2Cl_2 (δ 53.84). Melting points were measured using a Büchi Melting Point M-565 apparatus (sealed capillaries) and are uncorrected. High-resolution electrospray ionization (ESI) mass spectrometry was carried out using a Bruker micrOTOF-Q instrument in positive ion mode (capillary potential of 4500 V). Infrared spectra have been recorded on a Shimadzu FT-IR 8400S spectrophotometer. For alternative protocols and control reactions for **4**, **8**, and **9**, see the Supporting Information.

(2-Azidophenylisonitrile)(1,2,3,4,5-pentamethylcyclopentadienyl)iridium(III) Dichloride (2). An orange solution of $[IrCp^*Cl_2]_2$ (626 mg, 0.79 mmol, 1.0 equiv) in DCM (85 mL) was added to 2-azidophenyl isonitrile (252 mg, 1.75 mmol, 2.2 equiv) to provide a reddish brown solution which was stirred for 42 h at room temperature, in the absence of light. Evaporation provided a yellowish brown powder, which was washed with Et_2O (2 × 15 mL) to provide [(2-azidophenylisonitrile)$IrCp^*Cl_2$] as a yellow powder (835 mg, 1.54 mmol, 98.1%). [(2-azidophenylisonitrile)$IrCp^*Cl_2$] is light-sensitive in solution and was stored as a solid in the absence of light at −20 °C. Mp: 160 °C dec. ^{1}H NMR (500.23 MHz, $CDCl_3$): δ 7.46 (dd, $^3J_{H,H}$ = 8.1 Hz, $^4J_{H,H}$ = 1.3 Hz, 1H, *o*-Ar-*H*), 7.43 (td, $^3J_{H,H}$ = 8.0 Hz, $^4J_{H,H}$ = 1.5 Hz, 1H, *m*-Ar-*H*), 7.24 (dd, $^3J_{H,H}$ = 8.3 Hz, $^4J_{H,H}$ = 1.0 Hz, 1H *m*-Ar-*H*), 7.17 (td, $^3J_{H,H}$ = 7.9 Hz, $^4J_{H,H}$ = 1.1 Hz, 1H, *p*-Ar-*H*), 1.90 (s, 15H, Cp-CH_3). $^{13}C\{^1H\}$ NMR (125.78 MHz, $CDCl_3$): δ 137.5 (s, *m*-Ar-C-N_3), 130.7 (s, *o*-Ar-CH), 128.7 (s, *m*-Ar-CH), 125.5 (s, *m*-Ar-CH), 119.0 (s, *p*-Ar-CH), 95.3 (s, Cp*-CCH_3), 9.3 (s, Cp*-CCH_3), signals for Ar-*C*NC and Ar−*C*NC are unresolved. FT-IR: ν 3086 (w), 3015 (w), 3001 (w), 2966 (w), 2363 (w), 2164 (s), 2129 (s), 2054 (w), 2041 (w), 2015 (w), 2000 (w), 1616 (w), 1578 (w), 1489 (m), 1452 (w), 1441 (w), 1423 (w), 1404 (w), 1377 (w), 1312 (m), 1292 (w), 1283 (w), 1263 (w), 1209 (w), 1148 (w), 1092 (w), 1082 (w), 1024 (w), 962 (w), 831 (w), 798 (w), 779 (m), 756 (w), 733 (w), 704 (w), 687 (w), 650 (w), 619 (w), 577 (m), 544 (w), 530 (w), 517 (w), 474 (w), 449 (m), 420 (w) cm^{-1}. MS (ESI-Q-TOF): calcd for $C_{17}H_{19}N_4IrCl$, 507.0922; found, 507.0879.

(2-Azidophenylisonitrile)(1,2,3,4,5-pentamethylcyclopentadienyl)iridium(III) Diiodide (3). [(2-azidophenylisonitrile)-$IrCp^*Cl_2$] (298 mg, 0.55 mmol, 1.0 equiv) and NaI (1.5 g, 10 mmol, 18.0 equiv) were dissolved in acetone (20 mL) to provide an orange solution, which was stirred for 48 h at room temperature, in the absence of light. The resulting orange suspension was evaporated to provide a red residue, which was repeatedly extracted with DCM until colorless extracts were obtained (approximately 4 × 4 mL). Evaporation of the combined extracts yielded [(2-azidophenylisonitrile)$IrCp^*I_2$] as a dark orange-red solid (335 mg, 0.46 mmol, 84%). [(2-azidophenylisonitrile)$IrCp^*I_2$] is light-sensitive in solution and was stored as a solid in the absence of light at −20 °C. *Crystallization:* single crystals could be obtained by slow diffusion of pentane (4.5 mL/mmol of compound) into a DCM/pentane solution (27 mL of DCM + 9 mL of pentane/mmol of compound) at 5 °C. Mp: 145 °C dec. ^{1}H NMR (500.23 MHz, $CDCl_3$): δ 7.40 (dd, $^3J_{H,H}$ = 8.0 Hz, $J_{H,H}$ = 1.2 Hz, 1H, *o*-Ar-*H*), 7.36 (td, $^3J_{H,H}$ = 7.9 Hz, $J_{H,H}$ = 1.5 Hz, 1H, *m*-Ar-*H*), 7.21 (dd, $^3J_{H,H}$ = 8.3 Hz, $J_{H,H}$ = 0.9 Hz, 1H, *m*-Ar-*H*), 7.17 (td, $^3J_{H,H}$ = 7.8 Hz, $^4J_{H,H}$ = 1.1 Hz, 1H, *p*-Ar-*H*), 2.15 (s, 15H, Cp*-CH_3). $^{13}C\{^1H\}$ NMR (125.78 MHz, $CDCl_3$): δ 137.0 (s, *m*-Ar-*C*-N_3), 130.7 (s, *ipso*-Ar-*C*NC), 130.1 (s, *o*-Ar-CH), 128.7 (s, *m*-Ar-CH), 125.2 (s, *m*-Ar-CH), 118.9 (s, *p*-Ar-CH), 96.0 (Cp*-CCH_3), 10.6 (Cp*-CCH_3), the signal for Ar-*C*NC is unresolved. FT-IR: ν 2962 (w), 2916 (w), 2858 (w), 2357 (w), 2349 (w), 2326 (w), 2287 (w), 2118 (s), 2095 (s), 1894 (w), 1578 (w), 1485 (m), 1443 (m), 1423 (w), 1373 (w), 1358 (w), 1312 (s), 1258 (s), 1211 (w), 1080 (m), 1018 (s), 949 (w), 864 (w), 798 (s), 764 (s), 710 (w), 652 (m), 613 (w), 579 (s), 544 (m), 525 (m), 471 (m), 432 (m) cm^{-1}. MS (ESI-Q-TOF): calcd for $C_{17}H_{19}N_4IrI$, 599.0284; found, 599.0249.

(1*H*-Benzimidazolylidene)(1,2,3,4,5-pentamethylcyclopentadienyl)iridium(III) Diiodide (4). NaI (236 mg, 1.58 mmol, 4.1 equiv) was dissolved in acetone (40 mL), after which it was added to $FeCl_3$ (113 mg, 0.70 mmol, 1.8 equiv) to provide a black suspension. Immediately afterward, a solution of [(2-azidophenylisonitrile)$IrCp^*Cl_2$] (207 mg, 0.38 mmol, 1.0 equiv) in DCM (10 mL) was added to the black suspension and the resulting mixture was stirred for 43 h at room temperature, during which the mixture turned dark red. Volatiles (including iodine) were removed in vacuo to provide a very dark red residue, which was extracted in DCM (180 mL) under atmospheric conditions. The dark extract was subsequently washed with a solution of $Na_2S_2O_3$ (200 mL, 20% in H_2O), a solution of $NaHCO_3$ (200 mL, saturated solution in H_2O) and brine (200 mL). The resulting orange solution was dried over Na_2SO_4. After evaporation, [(1*H*-benzimidazolylidene)$IrCp^*I_2$] was obtained as a yellow powder (233 mg, 0.33 mmol, 87%). *Crystallization*: single crystals could be obtained by slow diffusion of pentane into a DCM solution (pentane/DCM approximately 1/3). Mp: 330 °C dec. ^{1}H NMR (500.23 MHz, CD_2Cl_2): δ 9.88 (s, 2H, N-*H*), 7.47−7.42 (m, 2H, Ar-*H*), 7.27−7.22 (m, 2H, Ar-*H*), 1.92 (s, 15H, Cp*-CH_3). $^{13}C\{^1H\}$ NMR (125.78 MHz, CD_2Cl_2): δ 161.0 (s, NCN), 134.2 (s, Ar-C), 123.8 (s, Ar-CH), 111.3 (s, Ar-CH), 91.6 (s, Cp*-CCH_3), 10.4 (s, Cp*-CCH_3). FT-IR: ν 3275 (w), 2962 (m), 2905 (w), 2380 (w), 1720 (w), 1616 (w), 1489 (w), 1450 (s), 1350 (m), 1304 (w), 1258 (s), 1153 (w), 1076 (s), 1011 (s), 864 (m), 791 (s), 729 (s), 706 (m), 675 (m), 636 (w), 602 (w), 532 (w), 494 (w) cm^{-1}. MS (ESI-Q-TOF): calcd for $C_{17}H_{21}IN_2Ir$, 573.0373; found, 573.0376.

(1*H*-Benzimidazolylidene)(1,2,3,4,5-pentamethylcyclopentadienyl)iridium(III) Dichloride (5). To an orange solution of [(1*H*-benzimidazolylidene)$IrCp^*I_2$] (69 mg, 0.098 mmol, 1.0 equiv) in THF (14 mL) was added AgOTf (53 mg, 0.206 mmol, 2.1 equiv) to provide a yellow suspension, which was stirred for 40 min at room temperature, in the absence of light. $Et_3N{\cdot}HCl$ (36 mg, 0.262 mmol, 2.7 equiv) was added to provide an orange-yellow solution, which was stirred for 120 min at room temperature. Filtration provided a yellow solution, which was evaporated. The resulting yellow solid was redissolved in DCM (40 mL) and washed with H_2O (2 × 40 mL). The yellow organic layer was dried with $MgSO_4$ and evaporated to provide an orange-yellow solid. Crystallization by cooling a DCM/pentane solution (20 mL/20 mL) to −80 °C provided pure [(1*H*-

DOI: 10.1021/acs.organomet.9b00584
Organometallics 2019, 38, 4543−4553

benzimidazolylidene)IrCp*Cl_2] as an orange solid (17 mg, 0.033 mmol, 34%). Mp: 289 °C dec. ^{1}H NMR (500.23 MHz, $CDCl_3$): δ 10.52 (s, 2H, N-*H*), 7.24−7.19 (m, 2H, Ar-*H*), 7.03−6.98 (m, 2H, Ar-*H*), 1.74 (s, 15H, Cp*-CH_3). ^{13}C{^{1}H} NMR (125.78 MHz, CD_2Cl_2): δ 165.7 (s, NCN), 133.5 (s, Ar-C), 123.4 (s, Ar-CH), 111.5 (s, Ar-CH), 90.0 (s, Cp*-CCH_3), 9.1 (s, Cp*-CCH_3). FT-IR: ν 3271 (w), 3204 (w), 2962 (w), 2907 (w), 2853 (w), 1655 (w), 1618 (w), 1618 (w), 1491 (w), 1456 (s), 1400 (w), 1362 (m), 1348 (m), 1259 (s), 1246 (m), 1151 (w), 1080 (s), 1014 (s), 864 (w), 795 (s), 756 (s), 743 (s), 700 (m), 681 (s), 662 (m), 638 (w), 621 (m), 586 (w), 563 (w), 486 (w), 459 (m), 447 (s), 434 (m), 401 (s) cm^{-1}. MS (ESI-Q-TOF): calcd for $C_{17}H_{21}ClN_2Ir$, 481.1009; found, 481.1013.

(*N*,*N*′-Dimethyl-2-benzimidazolylidene)(1,2,3,4,5-pentamethylcyclopentadienyl)iridium(III) Dichloride. To an orange solution of [IrCp*Cl_2]$_2$ (79.7 mg, 0.10 mmol, 1.0 equiv) in toluene (1 mL) was added a yellow solution of bis(1,3-dimethylbenzimidazolidin-2-ylidene) (29.2 mg, 0.10 mmol, 1.0 equiv) in toluene (1 mL). The reaction mixture was stirred for 4 h at 100 °C. The mixture was cooled to room temperature and stirred for 2 days to provide a yellow suspension. Filtration provided a yellow solid, which was washed with diethyl ether (3 × 2 mL) to provide (*N*,*N*′-dimethyl-2-benzimidazolylidene)IrCp*Cl_2 as a yellow solid (95 mg, 17.44 mmol, 88%). Mp: 244 °C dec. ^{1}H NMR (400.13 MHz, $CDCl_3$): δ 7.40−7.35 (m, 2H, Ar-*H*), 7.33−7.27 (m, 2H, Ar-*H*), 4.17 (s, 6H, N-CH_3), 1.68 (s, 15H, Cp*-CH_3). ^{13}C{^{1}H} NMR (100.61 MHz, $CDCl_3$): δ 170.6 (s, NCN), 135.9 (s, Ar-*C*), 123.5 (s, Ar-CH), 110.3 (s, Ar-CH), 89.6 (s, Cp*-CCH_3), 35.6 (s, N-CH_3), 9.3 (s, Cp*-CCH_3). FT-IR: ν 3990 (w), 3042 (w), 3028 (w), 2978 (w), 2953 (w), 2912 (w), 2897 (w), 1610 (w), 1508 w), 1489 (w), 1458 (m), 1445 (m), 1400 (w), 1375 (m), 1344 (m), 1250 (w), 1155 (w), 1136 (w), 1094 (m), 1078 (w), 1030 (w), 1013 (w), 955 (w), 808 (w), 795 (w), 768 (s), 696 (w), 681 (w), 613 (w), 567 (w), 532 (w), 469 (w), 447 (w), 434 (w), 417 (w), 401 (w) cm^{-1}. MS (ESI-Q-TOF): calcd for $C_{19}H_{25}ClN_2Ir$, 509.1330; found, 509.1330.

(*N*,*N*′-Dimethyl-2-benzimidazolylidene)(1,2,3,4,5-pentamethylcyclopentadienyl)iridium(III) Diiodide (6). To a yellow suspension of (*N*,*N*′-dimethyl-2-benzimidazolylidene)-IrCp*Cl_2 (71 mg, 0.13 mmol, 1.0 equiv) in acetone (10 mL) was added a solution of NaI (1.0 g, 6.67 mmol, 51 equiv) in acetone (15 mL) to provide a red-orange suspension which was stirred for 22 h at room temperature. Evaporation provided an orange solid, which was extracted into DCM (3 × 10 mL). Evaporation provided an orange-red solid, which was washed with pentane (20 mL) to provide (*N*,*N*′-dimethyl-2-benzimidazolylidene)IrCp*I_2 as an orange solid (95 mg, 0.13 mmol, quant.). *Crystallization*: single crystals could be obtained by cooling a saturated solution in DCM/pentane (1/1) to 5 °C. Mp: 270 °C decomp. ^{1}H NMR (500.23 MHz, $CDCl_3$): δ 7.37−7.32 (m, 2H, Ar-*H*), 7.31−7.27 (m, 2H, Ar-*H*), 4.16 (s, 6H, N-CH_3), 1.88 (s, 15H, Cp*-CH_3). ^{13}C{^{1}H} NMR (125.78 MHz, $CDCl_3$): δ 167.0 (s, NCN), 135.8 (s, Ar-C), 123.6 (s, Ar-CH), 110.4 (s, Ar-CH), 90.8 (s, Cp*-CCH_3), 40.6 (s, N-CH_3), 10.7 (s, Cp*-CCH_3). FT-IR: ν 3989 (w), 3049 (w), 2961 (w), 2934 (w), 2907 (w), 2853 (w), 2841 (w), 1686 (w), 1487 (w), 1456 (m), 1433 (m), 1396 (w), 1366 (m), 1339 (m), 1259 (m), 1242 (m), 1155 (w), 1132 (w), 1082 (s), 1013 (s), 933 (w), 864 (w), 797 (s), 746 (s), 700 (w), 675 (w), 662 (w), 633 (w), 611 (w), 588 (w), 565 (m), 534 (w), 492 (w), 438 (w), 403 (m) cm^{-1}. MS (ESI-Q-TOF): calcd for $C_{19}H_{25}IN_2Ir$, 601.0686; found, 601.0691.

(κ^2-*C*,*N*-1-(Acetimino)benzimidazolylidene)(1,2,3,4,5-pentamethylcyclopentadienyl)iridium(III) Diiodide (7). To [(1*H*-benzimidazolylidene)IrCp*I_2] (0.05 g, 0.07 mmol) was added MeCN (20 mL). The resulting yellow mixture was stirred for 24 h at reflux and 70 h at room temperature. Evaporation provided (κ^2-*C*,*N*-1-(acetimino)benzimidazolylidene)(1,2,3,4,5-pentamethylcyclopentadienyl)iridium(III) diiodide as a pale yellow solid (quantitative), which due to its unstable nature was used directly without further purification. Mp: 194 °C dec. ^{1}H NMR (500.23 MHz, CD_2Cl_2): δ 13.08 (s, 1H, Ir-N(*H*)C-CH_3), 10.88 (s, 1H, Ar-N-*H*), 8.25 (d, 9.1 Hz, 1H, Ar-C*H*), 7.70 (d, 8.1 Hz, 1H, Ar-C*H*), 7.40 (t, 7.8 Hz, 1H, Ar-C*H*), 7.34 (t, 7.8 Hz, 1H, Ar-C*H*), 3.35 (s, 3H, Ir-N(H)C-CH_3), 2.16 (s, 15H, Cp*-CH_3). FT-IR: ν 3103 (w), 3053 (w), 2962 (m), 2939 (w), 2907 (w), 1636 (w), 1601 (w), 1501 (w), 1475 (m), 1460 (m), 1445 (m), 1410 (w), 1385 (w), 1296 (w), 1258 (s), 1238 (w), 1190 (w), 1165 (w), 1155 (w), 1082 (s), 1013 (s), 864 (w), 791 (s), 754 (s), 704 (m), 681 (m), 662 (m), 608 (m), 548 (w), 498 (m), 424 (m) cm^{-1}. MS (ESI-Q-TOF): calcd for $C_{19}H_{24}IN_3Ir$, 614.0639; found, 614.0668.

(κ^2-*C*,*N*-(Acetimidoyl)benzimidazolylidene)(1,2,3,4,5-pentamethylcyclopentadienyl)iridium(III) Iodide (8). $FeCl_3$ (121 mg, 0.75 mmol, 1.5 equiv) and NaI (750 mg, 5.0 mmol, 10.0 equiv) were dissolved in MeCN (20 mL) to provide a black mixture. Immediately afterward, a solution of [(2-azidophenylisonitrile)-IrCp*Cl_2] (270 mg, 0.5 mmol, 1.0 equiv) in DCM (6 mL) was added and the resulting black mixture was stirred for 48 h at room temperature. Volatiles (including iodine) were removed in vacuo to provide a black residue, which was extracted with DCM (70 mL) under atmospheric conditions. The extract was subsequently washed with a solution of $Na_2S_2O_3$ (100 mL, 20% in H_2O) and $NaHCO_3$ (100 mL, saturated solution in H_2O). The resulting yellow solution was dried over Na_2SO_4. After evaporation and washing with $CHCl_3$ (10 mL), [(κ^2-*C*,*N*-(acetimidoyl)-benzimidazolylidene)IrCp*I] was obtained as a yellow powder (232 mg, 0.38 mmol, 76%). Mp: 316 °C dec. ^{1}H NMR (500.23 MHz, CD_2Cl_2): δ 7.94 (s, 1H, N*H*), 7.54 (d, $^3J_{H,H}$ = 7.6 Hz, 1H, Ar-*H*), 7.48 (d, $^3J_{H,H}$ = 7.8 Hz, 1H, Ar-*H*), 7.23−7.18 (m, 1H, Ar-*H*), 7.06−7.01 (m, 1H, Ar-*H*), 3.00 (d, $^7J_{H,H}$ = 0.9 Hz, 3H, Ir-NC−CH_3), 1.94 (s, 15H, Cp*-CH_3). ^{13}C{^{1}H} NMR (125.78 MHz, $CDCl_3$): δ 171.8 (s, NCN), 164.8 (s, Ir-NC-CH_3), 123.4 (s, Ar-CH), 121.1 (s, Ar-CH), 118.4 (s, Ar-CH), 110.1 (s, Ar-CH), 91.0 (s, Cp*-CCH_3), 19.8 (s, Ir-NC-CH_3) 9.58 (s, Cp*-CCH_3), signals for Ar-*C* are unresolved. FT-IR: ν 3132 (w), 3047 (w), 2974 (w), 2912 (w), 2862 (w), 2812 (w), 1620 (m), 1585 (w), 1493 (s), 1431 (s), 1373 (m), 1327 (w), 1292 (w), 1227 (m), 1184 (w), 1157 (w), 1126 (m), 1088 (m), 1022 (m), 987 (w), 910 (w), 810 (w), 752 (s), 737 (s), 710 (m), 687 (w), 663 (w), 617 (w), 552 (w), 498 (m), 432 (w) cm^{-1}. MS (ESI-Q-TOF): calcd for $C_{19}H_{24}IN_3Ir$, 614.0639; found, 614.0670.

Bis((1,2,3,4,5-pentamethylcyclopentadienyl)iridium(III)) μ-Hydrido Bis(μ,κ^2-*C*,*N*-1*H*-benzimidazolylidene) Chloride (9). [(2-azidophenylisonitrile)IrCp*Cl_2] (299 mg, 0.55 mmol, 1.0 equiv), NH_4Cl (130 mg, 2.43 mmol, 4.4 equiv), and zinc dust (90 mg, 1.38 mmol, 2.5 equiv) were combined in MeOH (60 mL) to give a yellow suspension, to which H_2O (0.6 mL) was added. The mixture was stirred at reflux for 166 h to provide a red solution, which was cooled to room temperature and was evaporated to give a red powder, which was washed with pentane (40 mL). Under atmospheric conditions, the powder was dissolved in DCM (120 mL) and washed with H_2O (6 × 50 mL). The organic layer was dried with Na_2SO_4, and the solvent was evaporated to provide a red powder, which was washed with Et_2O (3 × 30 mL) to yield [(μ,κ^2-*C*,*N*-1*H*-benzimidazolylidene)$_2$Ir$_2$Cp*$_2$(μ-H)Cl] as a red solid (198 mg, 0.21 mmol, 75%). *Crystallization:* crystallization by slow diffusion of Et_2O (5 mL) into a DCM (5 mL) solution at room temperature, provided [(μ,κ^2-*C*,*N*-1*H*-benzimidazolylidene)$_2$Ir$_2$Cp*$_2$(μ-H)Cl] as red needles (76 mg, 0.08 mmol, 30%). Single crystals were obtained by slow diffusion of Et_2O (0.6 mL) into a saturated solution of 1 equiv of [(μ,κ^2-*C*,*N*-1*H*-benzimidazolylidene)$_2$Ir$_2$Cp*$_2$(μ-H)Cl]/2 equiv of triphenylphosphane oxide in DCM (0.5 mL), buffered by a layer of DCM (0.1 mL) in an NMR tube. Mp: 212 °C dec. ^{1}H NMR (500.23 MHz, CD_2Cl_2): δ 12.37 (s, 2H, N*H*), 7.83 (d, $^3J_{HH}$ = 7.9 Hz, 2H, Ar Ir-NC-C*H*), 7.11 (d, $^3J_{HH}$ = 7.9 Hz, 2H, Ar HN-C-C*H*), 6.99 (t, $^3J_{HH}$ = 7.6 Hz, 2H, Ar Ir-NC-CH-C*H*), 6.86 (t, $^3J_{HH}$ = 7.6 Hz, 2H, Ar HN-C-CH-C*H*), 2.23 (s, 15H, C_2-Ir-Cp*-CH_3), 2.15 (s, 15H, N_2-Ir-Cp*-CH_3), −20.01 (s, 1H, Ir-*H*-Ir). ^{13}C{^{1}H} NMR (125.78 MHz, CD_2Cl_2): δ 142.2 (s, NCN), 141.5 (s, Ar Ir-NC-CH), 137.0 (s, Ar HN-C-CH), 120.4 (s, Ar Ir-NC-CH-*C*H), 120.0 (s, Ar N(H)C-CH-*C*H), 112.6 (s, Ar Ir-NC-*C*H), 111.7 (s, Ar N(H)C-*C*H), 94.4 (s, C_2-Ir-Cp*-*C*), 87.4 (s, N_2-Ir-Cp*-*C*), 11.8 (s, N_2-Ir-Cp*-CH_3), 10.9 (s, C_2-Ir-Cp*-CH_3). FT-IR: ν 3313 (w), 3252 (w), 3225 (w), 3117 (w), 3067 (w), 2962 (w), 2920 (w), 2854 (w), 1616 (w), 1450 (m), 1412 (m), 1369 (m), 1346 (w), 1292 (w), 1261 (m), 1219 (w), 1153

DOI: 10.1021/acs.organomet.9b00584
Organometallics 2019, 38, 4543−4553

(w), 1076 (m), 1026 (s), 980 (w), 868 (w), 798 (m), 744 (s), 698 (w), 617 (w), 575 (w), 536 (w), 498 (w), 436 (w) cm^{-1}. MS (ESI-Q-TOF): calcd for $C_{34}H_{41}N_4Ir_2$, 889.2561; found, 889.2586.

■ ASSOCIATED CONTENT

Supporting Information

The Supporting Information is available free of charge on the ACS Publications website at DOI: 10.1021/acs.organomet.9b00584.

Additional synthetic details, control experiments, NMR spectra, and geometries of computed structures (PDF)
Cartesian coordinates for calculated structures (XYZ)

Accession Codes

CCDC 1915713−1915715 and 1921152 contain the supplementary crystallographic data for this paper. These data can be obtained free of charge via www.ccdc.cam.ac.uk/data_request/cif, or by emailing data_request@ccdc.cam.ac.uk, or by contacting The Cambridge Crystallographic Data Centre, 12 Union Road, Cambridge CB2 1EZ, UK; fax: +44 1223 336033.

■ AUTHOR INFORMATION

Corresponding Authors

*E-mail for J.C.S.: j.c.slootweg@uva.nl.
*E-mail for K.L.: k.lammertsma@vu.nl.

ORCID

Mark K. Rong: 0000-0001-7518-0833
J. Chris Slootweg: 0000-0001-7818-7766
Koop Lammertsma: 0000-0001-9162-5783

Present Address

⊥Van 't Hoff Institute for Molecular Sciences, University of Amsterdam, Science Park 904, 1098 XH Amsterdam, The Netherlands.

Notes

The authors declare no competing financial interest.

■ ACKNOWLEDGMENTS

This work was supported by the Council for Chemical Sciences of The Netherlands Organization for Scientific Research (NWO/CW). We thank T. van Dijk for measuring high-resolution mass spectra. 2-Azidophenyl isonitrile was kindly provided by Carolin A. Dumke and F. Ekkehardt Hahn (Institut für Anorganische und Analytische Chemie, WWU Münster, Corrensstr. 28/30, D-48149 Münster, Germany).

■ REFERENCES

(1) For reviews on N-heterocyclic carbenes, see: (a) Herrmann, W. A.; Köcher, C. N-Heterocyclic Carbenes. *Angew. Chem., Int. Ed. Engl.* **1997**, *36*, 2162−2187. (b) Herrmann, W. A. N-Heterocyclic Carbenes: A New Concept in Organometallic Catalysis. *Angew. Chem., Int. Ed.* **2002**, *41*, 1290−1309. (c) Dröge, T.; Glorius, F. The Measure of All Rings—N-Heterocyclic Carbenes. *Angew. Chem., Int. Ed.* **2010**, *49*, 6940−6952. (d) Díez-González, S.; Marion, N.; Nolan, S. P. N-Heterocyclic Carbenes in Late Transition Metal Catalysis. *Chem. Rev.* **2009**, *109*, 3612−3676. (e) Lappert, M. F. Contributions to the chemistry of carbenemetal chemistry. *J. Organomet. Chem.* **2005**, *690*, 5467−5473.

(2) For a review on carbenes (including NHCs), see: de Frémont, P.; Marion, N.; Nolan, S. P. Carbenes: Synthesis, properties, and organometallic chemistry. *Coord. Chem. Rev.* **2009**, *253*, 862−892.

(3) (a) Clark, G. R.; Roper, W. R.; Wright, A. H. Synthesis, structure, and reactions of $IrCl_3(CCl_2)(PPh_3)$, a compound with an iridium-carbon double bond ($L_nIr = CCl_2$). *J. Organomet. Chem.* **1982**, *236*, C7−C10. (b) Fehlhammer, W. P.; Beck, G. Reaktionen am koordinierten Trichlormethylisocyanid II. Cyclische Dithio- und Diaminocarbene. *J. Organomet. Chem.* **1989**, *369*, 105−116.

(4) For reviews on protic NHCs, see: (a) Hahn, F. E. Substrate Recognition and Regioselective Catalysis with Complexes Bearing NR, NH-NHC Ligands. *ChemCatChem* **2013**, *5*, 419−430. (b) Jahnke, M. C.; Hahn, F. E. Complexes with protic (NH, NH and NH, NR) N-heterocyclic carbene ligands. *Coord. Chem. Rev.* **2015**, *293*−*294*, 95−115.

(5) The classical N-substituted NHCs only occasionally display N-substituent "wingtip" activations. For more information, see: (a) Prinz, M.; Grosche, M.; Herdtweck, E.; Herrmann, W. A. Unsymmetrically Substituted Iridium(III)-Carbene Complexes by a CH-Activation Process. *Organometallics* **2000**, *19*, 1692−1694. (b) Semwal, S.; Ghorai, D.; Choudhury, J. Wingtip-Dictated Cyclometalation of N-Heterocyclic Carbene Ligand Framework and Its Implication toward Tunable Catalytic Activity. *Organometallics* **2014**, *33*, 7118−7124. (c) Scott, N. M.; Pons, V.; Stevens, E. D.; Heinekey, D. M.; Nolan, S. P. An Electron-Deficient Iridium(III) Dihydride Complex Capable of Intramolecular C-H Activation. *Angew. Chem., Int. Ed.* **2005**, *44*, 2512−2515. (d) Tang, C. Y.; Smith, W.; Thompson, A. L.; Vidovic, D.; Aldridge, S. Iridium-Mediated Borylation of Benzylic C-H Bonds by Borohydride. *Angew. Chem., Int. Ed.* **2011**, *50*, 1359−1362. (e) Nelson, D. J.; Egbert, J. D.; Nolan, S. P. Deuteration of boranes: catalysed versus non-catalysed processes. *Dalton Trans.* **2013**, *42*, 4105−4109. (f) Nelson, D. J.; Truscott, B. J.; Egbert, J. D.; Nolan, S. P. Exploring the Limits of Catalytic Ammonia-Borane Dehydrogenation Using a Bis(N-heterocyclic carbene) Iridium(III) Complex. *Organometallics* **2013**, *32*, 3769−3772. (g) Tang, C. Y.; Lednik, J.; Vidovic, D.; Thompson, A. L.; Aldridge, S. Responses to unsaturation in iridium mono (N-heterocyclic carbene) complexes: synthesis and oligomerization of $[LIr(H)_2Cl]$ and $[LIr(H)_2]^+$. *Chem. Commun.* **2011**, *47*, 2523−2525. (h) Fortman, G. C.; Jacobsen, H.; Cavallo, L.; Nolan, S. P. Catalytic deuteration of silanes mediated by N-heterocyclic carbene-Ir(III) complexes. *Chem. Commun.* **2011**, *47*, 9723−9725.

(6) For reviews on the potential of protic NHC cooperativity, see: (a) Kuwata, S.; Ikariya, T. β-Protic Pyrazole and N-Heterocyclic Carbene Complexes: Synthesis, Properties, and Metal−Ligand Cooperative Bifunctional Catalysis. *Chem. - Eur. J.* **2011**, *17*, 3542−3556. (b) Kuwata, S.; Ikariya, T. Metal−ligand bifunctional reactivity and catalysis of protic N-heterocyclic carbene and pyrazole complexes featuring β-NH units. *Chem. Commun.* **2014**, *50*, 14290−14300.

(7) For a review on cooperative systems, see for instance: Khusnutdinova, J. R.; Milstein, D. Metal−Ligand Cooperation. *Angew. Chem., Int. Ed.* **2015**, *54*, 12236−12273.

(8) (a) Meier, N.; Hahn, F. E.; Pape, T.; Siering, C.; Waldvogel, S. R. Molecular Recognition Utilizing Complexes with NH, NR-Stabilized Carbene Ligands. *Eur. J. Inorg. Chem.* **2007**, *2007*, 1210−1214. (b) Das, R.; Hepp, A.; Daniliuc, C. G.; Hahn, F. E. Synthesis of Complexes with Protic NH, NH-NHC Ligands via Oxidative Addition of 2-Halogenoazoles to Zero-Valent Transition Metals. *Organometallics* **2014**, *33*, 6975−6987.

(9) Araki, K.; Kuwata, S.; Ikariya, T. Isolation and Interconversion of Protic N-Heterocyclic Carbene and Imidazolyl Complexes: Application to Catalytic Dehydrative Condensation of *N*-(2-Pyridyl)-benzimidazole and Allyl Alcohol. *Organometallics* **2008**, *27*, 2176−2178.

(10) (a) Das, R.; Daniliuc, C. G.; Hahn, F. E. Oxidative Addition of 2-Halogenoazoles—Direct Synthesis of Palladium(II) Complexes Bearing Protic NH, NH-Functionalized NHC Ligands. *Angew. Chem., Int. Ed.* **2014**, *53*, 1163−1166. (b) Hahn, F. E.; Langenhahn, V.; Pape, T. Template synthesis of tungsten complexes with saturated N-heterocyclic carbene ligands. *Chem. Commun.* **2005**, 5390−5392. (c) Hahn, F. E.; García Plumed, C.; Münder, M.; Lügger, T. Synthesis of Benzannulated N-Heterocyclic Carbene Ligands by a Template Synthesis from 2-Nitrophenyl Isocyanide. *Chem. - Eur. J.* **2004**, *10*, 6285−6293. (d) Kösterke, T.; Pape, T.; Hahn, F. E. Synthesis of NHC Complexes by Oxidative Addition of 2-Chloro-N-methylbenzimidazole. *J. Am. Chem. Soc.* **2011**, *133*, 2112−2115.

DOI: 10.1021/acs.organomet.9b00584
Organometallics 2019, 38, 4543−4553

(11) (a) Hahn, F. E.; Langenhahn, V.; Lügger, T.; Pape, T.; Le Van, D. Template Synthesis of a Coordinated Tetracarbene Ligand with Crown Ether Topology. *Angew. Chem., Int. Ed.* **2005**, *44*, 3759−3763. (b) Schmidtendorf, M.; Pape, T.; Hahn, F. E. Stepwise Preparation of a Molecular Square from NR, NR- and NH, O-Substituted Dicarbene Building Blocks. *Angew. Chem., Int. Ed.* **2012**, *51*, 2195−2198. (c) Flores-Figueroa, A.; Pape, T.; Feldmann, K.-O.; Hahn, F. E. Template-controlled synthesis of a planar [16]ane-$P_2C^{NHC}_2$ macrocycle. *Chem. Commun.* **2010**, *46*, 324−326. (d) Kaufhold, O.; Stasch, A.; Pape, T.; Hepp, A.; Edwards, P. G.; Newman, P. D.; Hahn, F. E. Metal Template Controlled Formation of [11]ane-P_2C^{NHC} Macrocycles. *J. Am. Chem. Soc.* **2009**, *131*, 306−317.

(12) Kösterke, T.; Kösters, J.; Würthwein, E.-U.; Mück-Lichtenfeld, C.; Schulte to Brinke, C.; Lahoz, F.; Hahn, F. E. Synthesis of Complexes Containing an Anionic NHC Ligand with an Unsubstituted Ring-Nitrogen Atom. *Chem. - Eur. J.* **2012**, *18*, 14594−14598.

(13) (a) Ruiz, J.; Berros, Á.; Perandones, B. F.; Vivanco, M. NHC−manganese(I) complexes as carbene transfer agents. *Dalton Trans.* **2009**, 6999−7007. (b) Ruiz, J.; Sol, D.; van der Maelen, J. F.; Vivanco, M. Base-Promoted Transmetalation Reactions of Protic N-Heterocyclic Carbenes and Acyclic Diamino Carbenes from Mn^I to Au^I: A Mechanistic Study. *Organometallics* **2017**, *36*, 1035−1041.

(14) Fehlhammer, W. P.; Finck, W. Amin-Additionen an μ-(1,2-Diisocyanobenzol)-bis(chlorogold): Reaktionsbeteiligung der Isocyan-Nachbarfunktion und [Au]C-Übertragung. *J. Organomet. Chem.* **1991**, *414*, 261−270.

(15) Xiang, L.; Xiao, J.; Deng, L. Synthesis, Structure, and Reactivity of Organo-Iron(II) Complexes with N-Heterocyclic Carbene Ligation. *Organometallics* **2011**, *30*, 2018−2025.

(16) (a) Zanotto, L.; Bertani, R.; Michelin, R. A. Synthesis and Deprotonation Reactions of Neutral and Cationic Cyclic (Aminooxy)carbenes Derived from Platinum(II) Carbonyls. *Inorg. Chem.* **1990**, *29*, 3265−3268. (b) Bertani, R.; Mozzon, M.; Michelin, R. A.; Benetollo, F.; Bombieri, G.; Castilho, T. J.; Pombeiro, A. J. L. Synthesis, chemical and electrochemical deprotonation reactions of aminocarbene complexes of palladium(II) and platinum(II). X-ray structure of $\{(PPh_3)ClPt[\mu\text{-}COCH_2CH_2N\text{-}C, N]\}_2$. *Inorg. Chim. Acta* **1991**, *189*, 175−187. (c) Poulain, A.; Neels, A.; Albrecht, M. Palladium Complexes Containing Potentially Chelating Pyridylidene-Type Carbene Ligands. *Eur. J. Inorg. Chem.* **2009**, *2009*, 1871−1881.

(17) (a) Steinhagen, H.; Helmchen, G. Asymmetric Two-Center Catalysis - Learning from Nature. *Angew. Chem., Int. Ed. Engl.* **1996**, *35*, 2339−2342. (b) Ma, J.-A.; Cahard, D. Towards Perfect Catalytic Asymmetric Synthesis: Dual Activation of the Electrophile and the Nucleophile. *Angew. Chem., Int. Ed.* **2004**, *43*, 4566−4583. (c) Rowlands, G. J. Ambifunctional cooperative catalysts. *Tetrahedron* **2001**, *57*, 1865−1882.

(18) Miranda-Soto, V.; Grotjahn, D. B.; Cooksy, A. L.; Golen, J. A.; Moore, C. E.; Rheingold, A. L. A Labile and Catalytically Active Imidazol-2-yl Fragment System. *Angew. Chem., Int. Ed.* **2011**, *50*, 631−635.

(19) Miranda-Soto, V.; Grotjahn, D. B.; DiPasquale, A. G.; Rheingold, A. L. Imidazol-2-yl Complexes of Cp*Ir as Bifunctional Ambident Reactants. *J. Am. Chem. Soc.* **2008**, *130*, 13200−13201.

(20) (a) Tan, K. L.; Bergman, R. G.; Ellman, J. A. Intermediacy of an N-Heterocyclic Carbene Complex in the Catalytic C-H Activation of a Substituted Benzimidazole. *J. Am. Chem. Soc.* **2002**, *124*, 3202−3203. (b) Wiedemann, S. H.; Lewis, J. C.; Ellman, J. A.; Bergman, R. G. Experimental and Computational Studies on the Mechanism of N-Heterocycle C-H Activation by Rh(I). *J. Am. Chem. Soc.* **2006**, *128*, 2452−2462. (c) Lewis, J. C.; Berman, A. M.; Bergman, R. G.; Ellman, J. A. Rh(I)-Catalyzed Arylation of Heterocycles via C-H Bond Activation: Expanded Scope through Mechanistic Insight. *J. Am. Chem. Soc.* **2008**, *130*, 2493−2500.

(21) For more information on NHC^H/imidazole tautomerization, see for instance: (a) Burling, S.; Mahon, M. F.; Powell, R. E.; Whittlesey, M. K.; Williams, J. M. J. Ruthenium Induced C-N Bond Activation of an N-Heterocyclic Carbene: Isolation of C- and N-Bound Tautomers. *J. Am. Chem. Soc.* **2006**, *128*, 13702−13703. (b) Sini, G.; Eisenstein, O.; Crabtree, R. H. Preferential C-Binding versus N-Binding in Imidazole Depends on the Metal Fragment Involved. *Inorg. Chem.* **2002**, *41*, 602−604. (c) Tonner, R.; Heydenrych, G.; Frenking, G. Bonding Analysis of N-Heterocyclic Carbene Tautomers and Phosphine Ligands in Transition-Metal Complexes: A Theoretical Study. *Chem. - Asian J.* **2007**, *2*, 1555−1567.

(22) Wang, X.; Chen, H.; Li, X. Ir(III)-Induced C-Bound to N-Bound Tautomerization of a N-Heterocyclic Carbene. *Organometallics* **2007**, *26*, 4684−4687.

(23) For more information on Ir(III) in hydroamination, see for instance: (a) Kashiwame, Y.; Kuwata, S.; Ikariya, T. Metal−Pyrazole Bifunction in Half-Sandwich C_N Chelate Iridium Complexes: Pyrazole−Pyrazolato Interconversion and Application to Catalytic Intramolecular Hydroamination of Aminoalkene. *Chem. - Eur. J.* **2010**, *16*, 766−770. (b) Tobisch, S. Metal−Ligand Cooperation in Catalytic Intramolecular Hydroamination: A Computational Study of Iridium−Pyrazolato Cooperative Activation of Aminoalkenes. *Chem. - Eur. J.* **2012**, *18*, 7248−7262. (c) Specht, Z. G.; Cortes-Llamas, S. A.; Tran, H. N.; van Niekerk, C. J.; Rancudo, K. T.; Golen, J. A.; Moore, C. E.; Rheingold, A. L.; Dwyer, T. J.; Grotjahn, D. B. Enabling Bifunctionality and Hemilability of N-Heteroaryl NHC Complexes. *Chem. - Eur. J.* **2011**, *17*, 6606−6609. (d) Gray, K.; Page, M. J.; Wagler, J.; Messerle, B. A. Iridium(III) Cp* Complexes for the Efficient Hydroamination of Internal Alkynes. *Organometallics* **2012**, *31*, 6270−6277. (e) Kashiwame, Y.; Kuwata, S.; Ikariya, T. Catalytic Intramolecular Hydroamination with a Bifunctional Iridium Pyrazolato Complex: Substrate Scope and Mechanistic Elucidation. *Organometallics* **2012**, *31*, 8444−8455. (f) Kumaran, E.; How, K. T. S.; Ganguly, R.; Li, Y.; Leong, W. K. Synthesis and Reactivity of Cationic Iridium Aminocarbenes Derived from Terminal Alkynes and 2-Aminopyridines. *Organometallics* **2013**, *32*, 4149−4152.

(24) Also rhenium(I)-pyrazolato complexes are known to exhibit similar MeCN hydroaminations: Gómez-Iglesias, P.; Arroyo, M.; Bajo, S.; Strohmann, C.; Miguel, D.; Villafañe, F. Pyrazolylamidino Ligands from Coupling of Acetonitrile and Pyrazoles: A Systematic Study. *Inorg. Chem.* **2014**, *53*, 12437−12448.

(25) See for instance: (a) Alcarazo, M.; Stork, T.; Anoop, A.; Thiel, W.; Fürstner, A. Steering the Surprisingly Modular π-Acceptor Properties of N-Heterocyclic Carbenes: Implications for Gold Catalysis. *Angew. Chem., Int. Ed.* **2010**, *49*, 2542−2546. (b) Collins, M. S.; Rosen, E. L.; Lynch, V. M.; Bielawski, C. W. Differentially Substituted Acyclic Diaminocarbene Ligands Display Conformation-Dependent Donicities. *Organometallics* **2010**, *29*, 3047−3053. (c) Back, O.; Henry-Ellinger, M.; Martin, C. D.; Martin, D.; Bertrand, G. ^{31}P NMR Chemical Shifts of Carbene−Phosphinidene Adducts as an Indicator of the π-Accepting Properties of Carbenes. *Angew. Chem., Int. Ed.* **2013**, *52*, 2939−2943. (d) Mercs, L.; Labat, G.; Neels, A.; Ehlers, A.; Albrecht, M. Piano-Stool Iron(II) Complexes as Probes for the Bonding of N-Heterocyclic Carbenes: Indications for π-Acceptor Ability. *Organometallics* **2006**, *25*, 5648−5656.

(26) Sanford, M. S.; Ulman, M.; Grubbs, R. H. New Insights into the Mechanism of Ruthenium-Catalyzed Olefin Metathesis Reactions. *J. Am. Chem. Soc.* **2001**, *123*, 749−750.

(27) Aktas, H.; Slootweg, J. C.; Schakel, M.; Ehlers, A. W.; Lutz, M.; Spek, A. L.; Lammertsma, K. N-Heterocyclic Carbene-Functionalized Ruthenium Phosphinidenes: What a Difference a Twist Makes. *J. Am. Chem. Soc.* **2009**, *131*, 6666−6667.

(28) For a review on (nucleophilic) phosphinidenes, see: (a) Aktas, H.; Slootweg, J. C.; Lammertsma, K. Nucleophilic Phosphinidene Complexes: Access and Applicability. *Angew. Chem., Int. Ed.* **2010**, *49*, 2102−2113. (b) Lammertsma, K. Phosphinidenes. *Top. Curr. Chem.* **2003**, *229*, 95−119.

(29) Method: BP86/ZORA/TZP, using ADF 2005.01b and 2005.01.[27]

(30) Iridium phosphinidene complexes are more stable than their Ru analogues. Termaten, A. T.; Schakel, M.; Ehlers, A. W.; Lutz, M.; Spek, A. L.; Lammertsma, K. N-Heterocyclic Carbene Functionalized Iridium Phosphinidene Complex [Cp*(NHC)Ir = PMes*]: Compar-

DOI: 10.1021/acs.organomet.9b00584
Organometallics 2019, 38, 4543−4553

ison of Phosphinidene, Imido, and Carbene Complexes. *Chem. - Eur. J.* **2003**, *9*, 3577−3582.
(31) Method: BP86/ZORA/TZ2P,32 using ADF2010.02.33. See the Supporting Information.
(32) (a) van Lenthe, E.; Baerends, E. J. Optimized Slater-type basis sets for the elements 1−118. *J. Comput. Chem.* **2003**, *24*, 1142−1156. (b) van Lenthe, E.; Baerends, E. J.; Snijders, J. G. Relativistic regular two-component Hamiltonians. *J. Chem. Phys.* **1993**, *99*, 4597−4610. (c) van Lenthe, E.; Baerends, E. J.; Snijders, J. G. Relativistic total energy using regular approximations. *J. Chem. Phys.* **1994**, *101*, 9783−9792. (d) van Lenthe, E.; Ehlers, A.; Baerends, E. J. Geometry optimizations in the zero order regular approximation for relativistic effects. *J. Chem. Phys.* **1999**, *110*, 8943−8953.
(33) (a) te Velde, G.; Bickelhaupt, F. M.; Baerends, E. J.; Fonseca Guerra, C.; van Gisbergen, S. J. A.; Snijders, J. G.; Ziegler, T. Chemistry with ADF. *J. Comput. Chem.* **2001**, *22*, 931−967. (b) Fonseca Guerra, C.; Snijders, J. G.; te Velde, G.; Baerends, E. J. Towards an order-N DFT method. *Theor. Chem. Acc.* **1998**, *99*, 391−403. (c) *ADF2010/2013/2016*; SCM, Theoretical Chemistry, Vrije Universiteit: Amsterdam, The Netherlands; http://www.scm.com.
(34) Kaufhold, O.; Flores-Figueroa, A.; Pape, T.; Hahn, F. E. Template Synthesis of Ruthenium Complexes with Saturated and Benzannulated NH, NH-Stabilized N-Heterocyclic Carbene Ligands. *Organometallics* **2009**, *28*, 896−901.
(35) Hahn, F. E.; Langenhahn, V.; Meier, N.; Lügger, T.; Fehlhammer, W. P. Template Synthesis of Benzannulated N-Heterocyclic Carbene Ligands. *Chem. - Eur. J.* **2003**, *9*, 704−712.
(36) (a) Jones, W. D.; Duttweiler, R. P., Jr.; Feher, F. J. Preparation and Characterization of $(C_5Me_5)Rh(CNR)_2$ and $[(C_5Me_5)Rh(CNR)]_2$ Complexes. *Inorg. Chem.* **1990**, *29*, 1505−1511. (b) Walsh, A. P.; Brennessel, W. W.; Jones, W. D. Synthesis and characterization of a series of rhodium, iridium, and ruthenium isocyanide complexes. *Inorg. Chim. Acta* **2013**, *407*, 131−138. (c) Suzuki, H.; Tajima, N.; Tatsumi, K.; Yamamoto, Y. Molecular architecture *via* coordination: quasi-octahedral macrocycles of rhodium and iridium bearing a pentamethylcyclopentadienyl group. *Chem. Commun.* **2000**, 1801−1802. (d) Saito, A.; Seino, H.; Kajitani, H.; Takagi, F.; Yashiro, A.; Ohnishi, T.; Mizobe, Y. Synthesis of sulfido- and thiolato-bridged Ir_3 cluster and its reactions with alkyne and isocyanide including highly regioselective cyclotrimerization of methyl propiolate. *J. Organomet. Chem.* **2006**, *691*, 5746−5752.
(37) Kamal, A.; Ramana, K. V.; Babu Ankati, H.; Ramana, A. V. Mild and efficient reduction of azides to amines: synthesis of fused [2,1-*b*]quinazolinones. *Tetrahedron Lett.* **2002**, *43*, 6861−6863.
(38) No details of the reduction mechanism have been reported.[37] We observed in situ iodine formation, as evidenced by purple fumes, when $FeCl_3$ and NaI were mixed, indicating the generation of I_2 and $FeCl_2$, which then performs the azide reduction. Hydrogen atom donation is assumed to take place during the aqueous workup.
(39) The same side reaction had been observed previously for Ru(II).[34] In the case of incomplete halogen exchange, the crude product was stirred with excess NaI in acetone at room temperature (Finkelstein conditions) to reach full conversion to **4**.
(40) Çetinkaya, E.; Hitchcock, P. B.; Küçükbay, H.; Lappert, M. F.; Al-Juaid, S. Carbene complexes XXIV. Preparation and characterization of two enetetramine-derived carbenerhodium(I) chloride complexes $RhCl(L^R)_3$ and $[RhCl(COD)L^R]$ (L^R = dCN(Me)Cu-$(CH)_4$Me-*o*) and the preparation and X-ray structures of the enetetramine $L^R{}_2$; and its salt $[L^R{}_2][BF_4]_2$. *J. Organomet. Chem.* **1994**, *481*, 89−95.
(41) Huynh, H. V.; Han, Y.; Jothibasu, R.; Yang, J. A. ^{13}C NMR Spectroscopic Determination of Ligand Donor Strengths Using N-Heterocyclic Carbene Complexes of Palladium(II). *Organometallics* **2009**, *28*, 5395−5404.
(42) For the molecular structure of (*N*,*N*′-dimethyl-2-benzimidazolylidene)IrCp*Cl_2, see: (a) Meredith, J. M.; Robinson, R., Jr.; Goldberg, K. I.; Kaminsky, W.; Heinekey, D. M. C-H Bond Activation by Cationic Iridium(III) NHC Complexes: A Combined Experimental and Computational Study. *Organometallics* **2012**, *31*, 1879−1887. (b) For molecular structures of related imidazol-2-ylidene-Ir(III) complexes, see ref 19 and: Hanasaka, F.; Fujita, K.-i.; Yamaguchi, R. Synthesis of New Cationic Cp*Ir N-Heterocyclic Carbene Complexes and Their High Catalytic Activities in the Oppenauer-Type Oxidation of Primary and Secondary Alcohols. *Organometallics* **2005**, *24*, 3422−3433 (c) For the molecular structure of the related $(NHC^H)Ru(II)(p\text{-cym})I_2$ complex, see ref 34..
(43) The symmetry operators for the respective I atoms are as follow: (i) $-x + 1, -y + 1, -z + 1$; (ii) $-x + 1, y - 1/2, -z + 3/2$. Similar NH- - -X interactions have been observed previously.[11d,34]
(44) Mitoraj, M. P.; Michalak, A.; Ziegler, T. A Combined Charge and Energy Decomposition Scheme for Bond Analysis. *J. Chem. Theory Comput.* **2009**, *5*, 962−975.
(45) The closely related complex (benzimidazolyl)IrCp*Cl_2 was synthetically confirmed to be highly insoluble (see the Supporting Information), and complexes akin to **7** are known to rearrange to their imidazolyl tautomers.[22]
(46) Although we are unaware of reports on iron(II)-based Ir(III) reductions, such a transformation might generate Ir(I), which upon oxidative N−H activation could eliminate HI to give the Ir(III) complex. Alternatively, iridium might be activated by a Lewis acidic Fe(III) species, which after iodide abstraction generates FeX_4 and a free coordination site. However, this is unlikely to lead to deprotonation, since a synthesis route toward a complex akin to the nondeprotonated **7** was reported by exploiting free coordination sites on iridium(III) (Scheme 3).[22]
(47) Nitriles can be activated for C-functionalization by (catalytic) acid, base, or alkylation. Nitrogen bases can stabilize nitrilium intermediates. For instance, see: (a) Pinner, A.; Klein, F. Umwandlung der Nitrile in Imide. IV: Mittheilung. *Ber. Dtsch. Chem. Ges.* **1878**, *11*, 1475−1487. (b) Schaefer, F. C.; Peters, G. A. Base-Catalyzed Reaction of Nitriles with Alcohols. A Convenient Route to Imidates and Amidine Salts. *J. Org. Chem.* **1961**, *26*, 412−418. (c) Rong, M. K.; van Duin, K.; van Dijk, T.; de Pater, J. J. M.; Deelman, B.-J.; Nieger, M.; Ehlers, A. W.; Slootweg, J. C.; Lammertsma, K. Iminophosphanes: Synthesis, Rhodium Complexes, and Ruthenium(II)-Catalyzed Hydration of Nitriles. *Organometallics* **2017**, *36*, 1079−1090. (d) van Dijk, T.; Bakker, M. S.; Holtrop, F.; Nieger, M.; Slootweg, J. C.; Lammertsma, K. Base-Stabilized Nitrilium Ions as Convenient Imine Synthons. *Org. Lett.* **2015**, *17*, 1461−1464.
(48) For a review on group IX hydroamination catalysts, see: Hesp, K. D.; Stradiotto, M. Rhodium- and Iridium-Catalyzed Hydroamination of Alkenes. *ChemCatChem* **2010**, *2*, 1192−1207.
(49) (a) Talwar, D.; Wu, X.; Saidi, O.; Salguero, N. P.; Xiao, J. Versatile Iridicycle Catalysts for Highly Efficient and Chemoselective Transfer Hydrogenation of Carbonyl Compounds in Water. *Chem. - Eur. J.* **2014**, *20*, 12835−12842. (b) Talwar, D.; Li, H. Y.; Durham, E.; Xiao, J. A Simple Iridicycle Catalyst for Efficient Transfer Hydrogenation of N-Heterocycles in Water. *Chem. - Eur. J.* **2015**, *21*, 5370−5379.
(50) (a) Randles, M. D.; Simpson, P. V.; Gupta, V.; Fu, J.; Moxey, G. J.; Schwich, T.; Criddle, A. L.; Petrie, S.; MacLellan, J. G.; Batten, S. R.; Stranger, R.; Cifuentes, M. P.; Humphrey, M. G. Syntheses of Pentanuclear Group 6 Iridium Clusters by Core Expansion of Tetranuclear Clusters with $Ir(CO)_2(\eta^5\text{-}C_5Me_4R)$ (R = H, Me). *Inorg. Chem.* **2013**, *52*, 11256−11268. (b) Tan, X.; Li, B.; Xu, S.; Song, H.; Wang, B. Synthesis, Reactivities, and Catalytic Properties of Iodo-Bridged Polymeric Iridium Complexes with Flexible Carbon Chain-Bridged Bis(tetramethylcyclopentadienyl) Ligands. *Organometallics* **2013**, *32*, 3253−3261. (c) Heinekey, D. M.; Millar, J. M.; Koetzle, T. F.; Payne, N. G.; Zilm, K. W. Structural and Spectroscopic Characterization of Iridium Trihydride Complexes: Evidence for Proton-Proton Exchange Coupling. *J. Am. Chem. Soc.* **1990**, *112*, 909−919. (d) Heinekey, D. M.; Fine, D. A.; Harper, T. G. P.; Michel, S. T. Dinuclear dihydride complexes of iridium: a study of structure and dynamics. *Can. J. Chem.* **1995**, *73*, 1116−1125. (e) Heinekey, D. M.; Hinkle, A. S.; Close, J. D. Quantum Mechanical Exchange Coupling in Iridium Trihydride Complexes. *J. Am. Chem. Soc.* **1996**, *118*, 5353−5361. (f) Paisner, S. N.; Lavoie, G. G.; Bergman, R. G.

DOI: 10.1021/acs.organomet.9b00584
Organometallics 2019, 38, 4543−4553

Formation of planar-chiral alkylphosphine- and aniline-substituted cyclopentadienyl metal complexes and their reactivity toward electrophiles. *Inorg. Chim. Acta* **2002**, *334*, 253−275.
(51) Flores-Figueroa, A.; Kaufhold, O.; Feldmann, K.-O.; Hahn, F. E. Synthesis of NHC complexes by template controlled cyclization of *β*-functionalized isocyanides. *Dalton Trans.* **2009**, 9334−9342.
(52) On the basis of the Ir−C and Ir−N distances, the ligand is described as an N-anionic NHC^{H}, rather than a C-anionic benzimidazole.
(53) See for instance: (a) White, C.; Oliver, A. J.; Maitlis, P. M. Pentamethylcyclopentadienyl-rhodium and -iridium Complexes. Part VII. Mono-, Di-, and Tri-*μ*-Hydrido-complexes. *J. Chem. Soc., Dalton Trans.* **1973**, 1901−1907. (b) Gill, D. S.; Maitlis, P. M. Pentamethylcyclopentadienyl-rhodium and − iridium complexes VIII. Di-*μ*-hydridobis[chloro(pentamethylcyclopentadienyl)iridium] and related compounds. *J. Organomet. Chem.* **1975**, *87*, 359−364.
(54) Fujita, K.-i.; Hamada, T.; Yamaguchi, R. dppm and hydrido-bridged dinuclear complexes of iridium. Synthesis and structures of $[(IrCp^*)_2(\mu\text{-dppm})(\mu\text{-H})(\mu\text{-X})]^{2+}$ (X = Cl, OMe, OH, or H). *J. Chem. Soc., Dalton Trans.* **2000**, 1931−1936.
(55) Sola, E.; Bakhmutov, V. I.; Torres, F.; Elduque, A.; López, J. A.; Lahoz, F. J.; Werner, H.; Oro, L. A. Cooperative Bimetallic Effects on New Iridium(III) Pyrazolate Complexes: Hydrogen-Hydrogen, Carbon-Hydrogen, and Carbon-Chlorine Bond Activations. *Organometallics* **1998**, *17*, 683−696.
(56) Padilla-Martínez, I. I.; Cervantes-Vásquez, M.; Leyva-Ramirez, M. A.; Paz-Sandoval, M. A. Iridaoxacyclohexadiene-Bridged Mixed-Valence Iridium Cyclooctadiene Complex: Oxidative Addition and Hydrogen-Transfer to Coordinated Cyclooctadiene. *Organometallics* **2014**, *33*, 6305−6318.
(57) Fujita, K.-i.; Takahashi, Y.; Nakaguma, H.; Hamada, T.; Yamaguchi, R. Activation of C−H and H−H bonds by dinuclear iridium complexes. Oxidative addition to highly active unsaturated $32e^-$ diiridium species. *J. Organomet. Chem.* **2008**, *693*, 3375−3382.
(58) (a) Etter, M. C.; Baures, P. W. Triphenylphosphine Oxide as a Crystallization Aid. *J. Am. Chem. Soc.* **1988**, *110*, 639−640. (b) Hahn, F. E.; Imhof, L. Reactions of 2-(Trimethylsiloxy)phenyl Isocyanide with Complexes of Rhenium in the + 1, + 3, and + 5 Oxidation States. *Organometallics* **1997**, *16*, 763−769.
(59) Cocrystallization with TPPO was expected to provide beneficial hydrogen-bonding interactions with the *N*−H atoms, but no TPPO was incorporated in the final structure.
(60) Orpen, A. G.; Brammer, L.; Allen, F. H.; Kennard, O.; Watson, D. G.; Taylor, R. Tables of Bond Lengths determined by X-Ray and Neutron Diffraction. Part 2. Organometallic Compounds and Co-ordination Complexes of the *d*- and f-Block Metals. *J. Chem. Soc., Dalton Trans.* **1989**, S1−S83.
(61) Bader, R. F. W. *Atoms In Molecules*; Clarendon Press: Oxford, U.K., 1994. (b) Rodríguez, J. I.; Bader, R. F. W.; Ayers, P. W.; Michel, C.; Götz, A. W.; Bo, C. A high performance grid-based algorithm for computing QTAIM properties. *Chem. Phys. Lett.* **2009**, *472*, 149−152. (c) Rodríguez, J. I. An efficient method for computing the QTAIM topology of a scalar field: The electron density case. *J. Comput. Chem.* **2013**, *34*, 681−686.
(62) Additionally, Ir(II) and Ir(IV) are paramagnetic species, which should have had a clear effect on the NMR spectroscopic data and no such effects were observed.
(63) Song, G.; Su, Y.; Periana, R. A.; Crabtree, R. H.; Han, K.; Zhang, H.; Li, X. Anion-Exchange-Triggered 1,3-Shift of an NH Proton to Iridium in Protic N-Heterocyclic Carbenes: Hydrogen-Bonding and Ion-Pairing Effects. *Angew. Chem., Int. Ed.* **2010**, *49*, 912−917.
(64) See for instance: (a) Su, Y.; Song, G.; Han, K.; Li, X. Theoretical studies of iridium-mediated tautomerization of substituted pyridines. *J. Organomet. Chem.* **2011**, *696*, 1640−1646. (b) He, F.; Braunstein, P.; Wesolek, M.; Danapoulos, A. A. Imine-functionalised protic NHC complexes of Ir: direct formation by C−H activation. *Chem. Commun.* **2015**, *51*, 2814−2817.
(65) Institut für Anorganische und Analytische Chemie, WWU Münster, Corrensstr. 28/30, D-48149 Münster, Germany.
(66) Ball, R. G.; Graham, W. A. G.; Heinekey, D. M.; Hoyano, J. K.; McMaster, A. D.; Mattson, B. M.; Michel, S. T. Synthesis and Structure of $[(\eta\text{-}C_5Me_5)Ir(CO)]_2$. *Inorg. Chem.* **1990**, *29*, 2023−2025.
(67) Bostai, B.; Novák, Z.; Bényei, A. C.; Kotschy, A. Quinoidal Tetrazines: Formation of a Fascinating Compound Class. *Org. Lett.* **2007**, *9*, 3437−3439.

DOI: 10.1021/acs.organomet.9b00584
Organometallics 2019, 38, 4543−4553